Predictions of Variable-Energy Blast Waves

Mark N. Director*
United Technologies Research Center, East Hartford, Conn.
and
Eli K. Dabora†
University of Connecticut, Storrs, Conn.

Results from a numerical investigation of spherical blast waves with time-dependent energy deposition are reported. A description of the dynamics of these "variable-energy" blast waves is obtained from the solution of a set of nonlinear, partial differential equations that represent the conservation of mass, momentum, and energy in a spherically symmetric flowfield. For the current application, a finite-difference formulation of the governing equations in Lagrangian coordinates was selected, and the time-dependent nature of energy deposited was restricted to a power law input with positive exponent. Numerical calculations were performed during the energy deposition period for linear energy deposition. Propagation and decay of the shock front as well as internal flowfield properties have been obtained for these blast waves in air and chloroform. Results presented include shock front trajectory and Mach number, and radial density and pressure profiles for linear energy deposition in air for the spherically symmetric case.

Nomenclature

a_∞ = speed of sound in undisturbed gas
c = constant used in artificial viscosity expression
e = internal energy per unit mass
e_∞ = internal energy per unit mass of undisturbed medium
$\bar{e}$ = nondimensional energy, e/e_∞
E = energy input
E_{tot} = total energy input
E_α = energy input per unit surface area of the shock wave at a shock radius of unity, E_{tot}/F_0
F_0 = dimensional constant: 1, 2π, 4π for planar, cylindrically symmetric, and spherically symmetric flows, respectively
i = subscript for mass in finite-difference approximation
J_0 = similarity integral from Refs. 2 and 12
m = mass
m_s = undisturbed mass contained within radius R_s, $F_0\rho_\infty R_{s0}^{\alpha+1}/(\alpha+1)$
m_0 = undisturbed mass contained within radius R_0, $F_0\rho_\infty R_0^{\alpha+1}/(\alpha+1)$
m_0' = revised mass, defined in Eq. (34)
$\bar{m}$ = nondimensional mass = m/m_s
M_s = shock Mach number
n = subscript for time in finite-difference approximation
p = pressure
p_∞ = pressure of undisturbed medium
$\bar{p}$ = nondimensional pressure, p/p_∞
q = artificial viscosity
$\bar{q}$ = nondimensional artificial viscosity, q/p_∞
r = radius
$\bar{r}$ = nondimensional radius, r/R_0
R_0 = explosion scale radius, defined in Eq. (11)
R_0' = revised explosion scale radius, defined in Eq. (32)
R_p = piston radius
R_{p0} = piston radius at time of similarity solution
R_s = shock radius
R_{s0} = shock radius at time of similarity solution
t = time
t_i = energy input time
u = velocity
$\bar{u}$ = nondimensional velocity, u/a_∞
v = specific volume, $1/\rho$
v_∞ = specific volume of undisturbed medium
$\bar{v}$ = nondimensional specific volume, v/v_∞
α = dimensional constant: 0, 1, 2 for planar, cylindrically symmetric, and spherically symmetric flows, respectively
β = exponent for energy deposition, $E \sim t^\beta$
γ = ratio of specific heats
ρ = density
ρ_∞ = density of undisturbed medium
$\bar{\rho}$ = nondimensional density, ρ/ρ_∞
τ = nondimensional time, ta_∞/R_0
τ' = revised nondimensional time, defined in Eq. (33)
τ_i = nondimensional energy input time, $t_i a_\infty/R_0$
τ_{sim} = nondimensional time when initial similarity solution is applied

Presented as Paper 76-400 at the AIAA 9th Fluid and Plasma Dynamics Conference, San Diego, Calif., July 14-16, 1976; submitted July 26, 1976; revision received May 20, 1977.

Index category: Shock Waves and Detonations.

*Research Engineer; presently Head, Gas Physics Section, Atlantic Research Corporation, Alexandria, Va. Member AIAA.

†Professor, Mechanical Engineering Department. Associate Fellow AIAA.

Introduction

THE classical blast wave theory generally refers to the propagation of shock waves in a gaseous medium as the result of an instantaneous release of energy in an infinitesimally small region. Energy release can occur in a plane, along a line, or at a point in space with the resultant shock wave and flowfield being planar, cylindrically symmetric, or spherically symmetric, respectively. Since the early work of Taylor,[1] a considerable number of publications on the subject have appeared in the literature, including treatises and reviews such as those of Sakurai,[2] Sedov,[3] and Lee et al.[4] The proliferation of analyses has resulted in different and sometimes confusing sets of nomenclatures. A systematic approach to the treatment of the relevant conservation equations where the nomenclature of various contributors is compared, as well as a comprehensive study of self-similar blast waves, is given by Oppenheim et al.[5,6]

Early analytical treatment of the subject made use of the assumptions that the energy input is instantaneous, that the ambient pressure is negligible compared to the shock overpressure (i.e., strong shock wave), and that transport properties are unimportant. With these assumptions, Sedov[3]

applied dimensional analysis to obtain a similarity solution of the flowfield. However, flowfield details at late times when the strong shock assumption is no longer valid cannot be determined without the use of numerical methods.

Although the assumption of instantaneous energy input is considered adequate for most problems, there are processes in which the energy input, though very rapid, should be considered to be time-dependent. Examples of time-dependent energy input are arc discharges, exploding wire phenomena, chemical energy release as might occur in two-phase detonations, and cw laser-driven blast waves. The last phenomenon has been analyzed by Boni,[7] who made use of a power-law density profile assumption previously found[8] to be reasonable for the instantaneous-energy blast wave.

A detailed analytical and experimental investigation of spherical blast waves resulting from linear time-dependent energy input was undertaken by Director.[9] The analytical aspects of the investigation are the basis for this paper, whereas the experimental findings have been presented elsewhere.[10] It should be pointed out that the similarity solutions for time-dependent energy input cases as presented by Rogers[11] and Dabora[12] indicate that blast waves resulting from linear time-dependent energy input are, in essence, "piston-driven" waves.

The analytical investigation to be presented is based upon a finite-difference formulation of the equations of motion. Inviscid equations of motion are cast in Lagrangian coordinates, where time and mass are considered to be the independent variables. Propagation and decay of the shock front, as well as the internal flowfield properties, are obtained in the solution.

Analytical Description and Results

Differential Equations

The equations of motion for flow of a one-dimensional, inviscid, compressible gas may be expressed conveniently in Eulerian coordinates as follows:

Conservation of Mass

$$\frac{\partial}{\partial t}(\rho r^{\alpha}) + \frac{\partial}{\partial r}(\rho r^{\alpha} u) = 0 \tag{1}$$

Conservation of Momentum

$$\frac{\partial}{\partial t}(\rho r^{\alpha} u) + \frac{\partial}{\partial r}\left\{\rho r^{\alpha}\left(u^2 + \frac{p}{\rho}\right)\right\} = \alpha p r^{\alpha-1} \tag{2}$$

Conservation of Energy

$$\frac{\partial}{\partial t}\left\{\rho r^{\alpha}\left(e + \frac{u^2}{2}\right)\right\} + \frac{\partial}{\partial r}\left(\rho r^{\alpha} u\left\{e + \frac{u^2}{2} + \frac{p}{\rho}\right\}\right) = 0 \tag{3}$$

where r and t are the independent space and time coordinates, ρ, u, p, and e are the dependent density, velocity, pressure, and internal energy variables, and $\alpha = 0$, 1, or 2 for planar, cylindrical, or spherical geometry, respectively. Energy addition is applied as a boundary condition at the inner boundary. The form of this boundary condition will be discussed later.

An equation of state such as

$$p = \rho e(\gamma - 1) \tag{4}$$

for a thermally perfect gas with a constant ratio of specific heats γ completes the set of equations.

The mass contained within any region of space adjacent to the origin is

$$m = F_0 \int_0^r \rho r^{\alpha} \mathrm{d}r \tag{5}$$

where $F_0 = 1$, 2π, or 4π for planar, cylindrical, or spherical geometry, respectively. Mass as just defined is understood to be the mass per unit area in planar geometry and mass per unit length in cylindrical geometry.

The conservation equations (1-3) are transformed to Lagrangian form using the relationship of Eq. (5). After simplification, the conservation equations can be expressed as follows:

$$\frac{\partial}{\partial t}(\rho r^{\alpha}) + F_0 \rho^2 r^{2\alpha} \frac{\partial u}{\partial m} = 0 \tag{6}$$

$$\frac{\partial u}{\partial t} + F_0 r^{\alpha} \frac{\partial (p+q)}{\partial m} = 0 \tag{7}$$

$$\frac{\partial (e + u^2/2)}{\partial t} + F_0 \frac{\partial}{\partial m}\left\{r^{\alpha} u (p+q)\right\} \tag{8}$$

Following Von Neumann and Richtmeyer,[13] an artificial viscous dissipation term has been added to the hydrodynamic pressure in the differential equations. This artificial viscosity q is used to spread a shock over several mass points, thus allowing integration of the equations through the normally discontinuous shock region. The artificial viscosity is formulated in a manner such that it disappears in noncompression regions.

Two additional equations are needed to solve for the five dependent variables; these are the definition of particle velocity:

$$u = \partial r / \partial t \tag{9}$$

and the equation of state, Eq. (4).

The Lagrangian equations are nondimensionalized by applying the following substitutions:

$$\tau = t\alpha_{\infty}/R_0, \quad \bar{m} = m/m_s, \quad \bar{r} = r/R_{s_0}, \quad \bar{u} = u/a_{\infty} \tag{10a}$$

$$\bar{\rho} = \rho/\rho_{\infty}, \quad \bar{p} = p/p_{\infty}, \quad \bar{q} = q/p_{\infty}, \quad \bar{e} = e/e_{\infty} \tag{10b}$$

In formulating these nondimensional variables, the characteristic explosion length[14,15] is used:

$$R_0 = \{E_{\alpha}/p_{\infty}\}^{1/(\alpha+1)} \tag{11}$$

In this expression, E_{α} is the total energy (E_{tot}) deposited during the input time t_i (τ_i in nondimensional form) divided by the geometric constant F_0, and p_{∞} is the ambient pressure. An equivalent shock mass[9] also is employed. This is defined as the mass of undisturbed gas contained within a radius equal to the shock radius at some arbitrary starting time (R_{s0}), so that

$$m_s = F_0 \int_0^{R_{s0}} \rho_{\infty} r^{\alpha} \mathrm{d}r = \frac{F_0}{\alpha+1} \rho_{\infty} R_{s0}^{\alpha+1} \tag{12}$$

Following substitution of the nondimensional terms, the governing equations become

$$\frac{\partial \bar{u}}{\partial \tau} = \frac{-(\alpha+1)}{\gamma} \frac{R_0}{R_{s0}} \bar{r}^{\alpha} \frac{\partial (\bar{p}+\bar{q})}{\partial \bar{m}} \tag{13}$$

$$\frac{\partial \bar{r}}{\partial \tau} = \frac{R_0}{R_{s0}} \bar{u} \tag{14}$$

$$\bar{\rho} = \left[(\alpha+1)\bar{r}^{\alpha} \frac{\partial \bar{r}}{\partial \bar{m}}\right]^{-1} = \left(\frac{\partial \bar{r}^{\alpha+1}}{\partial \bar{m}}\right)^{-1} \tag{15}$$

$$\frac{\partial \bar{e}}{\partial \tau} = (\gamma - 1)\left(\frac{\bar{p}+\bar{q}}{\bar{\rho}^2}\right) \frac{\partial \bar{\rho}}{\partial \tau} \tag{16}$$

$$\bar{p} = \bar{\rho}\bar{e} \tag{17}$$

Energy input normally is applied as a boundary condition at the inner boundary. The present numerical scheme makes use of the findings of several investigators[11,12] which indicate the existence of a "piston" at the inner boundary for flows with time-dependent energy deposition. This piston has been assumed in the present study to propagate at a rate dictated by the similarity condition:

$$R_p = R_{p0}(\tau/\tau_{\text{sim}})^{(\beta+2)/(\alpha+3)} \tag{18}$$

where R_p is the piston position at time τ, and R_{p0} is the piston position at the arbitrary starting time τ_{sim} when a similarity solution first is applied to obtain starting information for the finite-difference calculation.

The form of the artificial viscosity term of Von Neumann and Richtmeyer[13] now is specified. The artificial viscosity term, modified to account for arbitrary geometry, can be expressed as

$$q = -\rho\left(\frac{c\Delta m}{F_0 r^\alpha}\right)^2 \frac{\partial v}{\partial t}\left|\frac{\partial v}{\partial t}\right|; \quad \frac{\partial v}{\partial t} < 0 \tag{19a}$$

$$q = 0; \quad \frac{\partial v}{\partial t} \geq 0 \tag{19b}$$

Note that the artificial viscosity term deliberately is made nonzero only in compression regions. Using conservation of mass and noting that $v = 1/\rho$, Eq. (19) can be expressed in an alternative, nondimensional form as

$$\bar{q} = \gamma\bar{\rho}\left[\frac{c\Delta\bar{m}}{\bar{r}^\alpha}\frac{\partial}{\partial\bar{m}}(\bar{r}^\alpha\bar{u})\right]^2; \quad \frac{\partial(\bar{r}^\alpha\bar{u})}{\partial\bar{m}} < 0 \tag{20a}$$

$$\bar{q} = 0; \quad \frac{\partial(\bar{r}^\alpha\bar{u})}{\partial\bar{m}} \geq 0 \tag{20b}$$

Finite-Difference Equations

The governing equations can be expressed in finite-difference form using a modified central difference scheme based on the work of Brode.[16-18] Velocity, position, density (or specific volume), and pressure are identified at the time and mass points indicated in Fig. 1. With such an identification scheme, it is possible to translate the differential equations into finite-difference equations that deal with centered quantities, where each difference equation is balanced about a time and a mass point, thus reducing the numerical errors associated with the approximation of differential equations by finite differences.

Velocity at the new time, $n+1$, for each mass point is based upon known information at times n and $n-1$:

$$u_{i+1}^{n+1} = u_{i+1}^{n-1} - \frac{(\alpha+1)}{\gamma}\frac{R_0}{R_{s0}}\frac{\Delta\tau^n}{\Delta m_{i+1}}(r_{i+1}^n)^\alpha(p_{i+2}^n + q_{i+2}^{n-1} - p_i^n - q_i^{n-1}) \tag{21}$$

In this equation, subscripts $(i+2, i+1$, and $i)$ and superscripts $(n-1, n$, and $n+1)$ indicate definitions of each dependent variable at those discrete masses and times. The term R_{s0}, as used in this and subsequent equations, is the shock radius determined from a similarity solution at the arbitrary starting time of the computational scheme. Radii for the various mass points at time $n+2$ are calculated based upon the preceding velocities and the time increment $\Delta\tau^{n+1}$:

$$r_{i+1}^{n+2} = r_{i+1}^n + (R_0/R_{s0})\Delta\tau^{n+1}u_{i+1}^{n+1} \tag{22}$$

From the calculated radii at the new time step, the density and specific volume are determined:

$$\rho_i^{n+2} = \frac{\Delta m_i}{(r_{i+1}^{n+2})^{\alpha+1} - (r_{i-1}^{n+2})^{\alpha+1}} \tag{23}$$

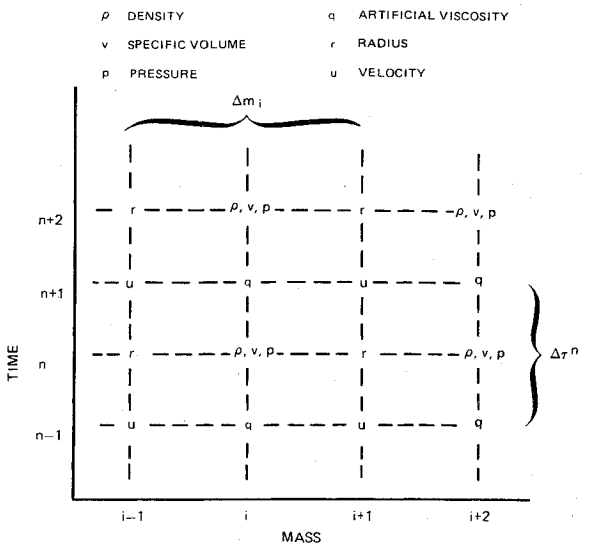

Fig. 1 Lagrangian difference grid.

and

$$v_i^{n+2} = 1/\rho_i^{n+2} \tag{24}$$

The aritificial viscosity is calculated at the new time step based upon the previously calculated variables:

$$q_i^{n+1} = \gamma\rho_i^{n+1}[\{c/(r_i^{n+1})^\alpha\}\{(r_{i+1}^{n+1})^\alpha u_{i+1}^{n+1} - (r_{i-1}^{n+1})^\alpha u_{i-1}^{n+1}\}]^2 \tag{25}$$

Finally, a new pressure is calculated from all of the preceding information:

$$p_i^{n+2} = \frac{\{p_i^n([(\gamma+1)/(\gamma-1)]\rho_i^{n+2} - \rho_i^n) + 2q_i^{n+1}(\rho_i^{n+2} - \rho_i^n)\}}{\{[(\gamma+1)/(\gamma-1)\rho_i^n - \rho_i^{n+2})\}} \tag{26}$$

Stability Requirements

Finite-difference methods usually are subject to mathematical limitations that place an upper bound on the size of the time increments that can be taken without incurring computational instabilities. The Courant stability condition[9,13] usually is applied to limit the time step. This condition is simply a statement that time steps should be smaller than the time required for a sound signal to propagate beyond the boundaries of adjacent zones.

A second stability consideration arises in compression regions, such as the shock front, where the presence of the quadratic artificial viscosity term changes the form of the linearized differential equations from wave-type equations to diffusion-type equations. In such high-compression regions, a diffusion stability condition must be met. Derivation of this artificial viscosity stability conditions is given in Ref. 9. In practice, the maximum time step allowed cannot exceed the smaller of either the Courant stability condition or the artificial viscosity condition, i.e., the lesser of the following:

Courant Stability

$$\Delta\tau \leq \left\{\left[\frac{R_{s0}/R_0}{(\alpha+1)(r_i^{n+2})^\alpha}\right]^2\frac{v_i^{n+2}}{p_i^{n+2}}\Delta m_i\right\}_{\min}^{1/2} \tag{27}$$

Artificial Viscosity Stability

$$\Delta\tau \leq \frac{v_i^{n+2}/R_{s0}/R_0/\Delta_{mi}}{4(\alpha+1)c^2(r_i^{n+2})^\alpha|u_{i+1}^{n+1} - u_{i-1}^{n+1}|}; \quad q_i^{n+1} \neq 0 \tag{28}$$

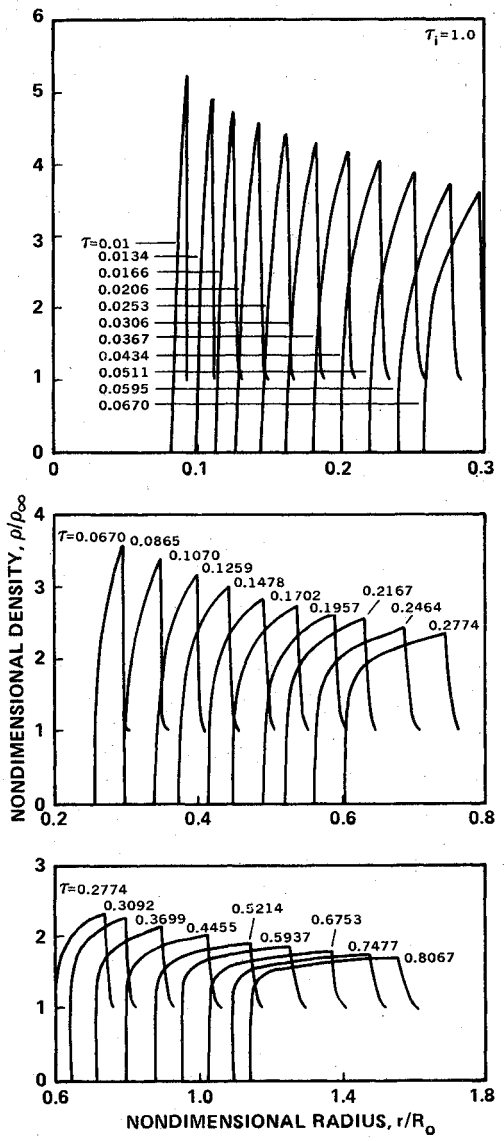

Fig. 2 Radial density profiles for linear energy input in air.

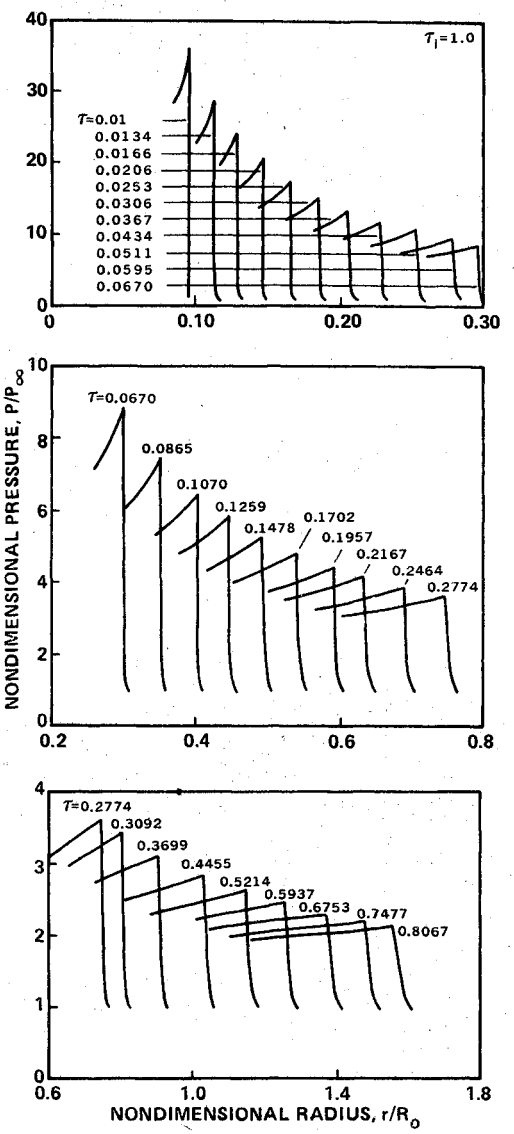

Fig. 3 Radial pressure profiles for linear energy input in air.

Computer Program Using the Finite-Difference Equations

The finite-difference formulation of the equations of motion in Lagrangian form discussed previously was programmed for solution on the IBM 360 digital computer. Starting information consisting of a complete specification of the flowfield at some point in time is obtained from a similarity solution. The similarity solution must be applied at a sufficiently high Mach number ($M \gg 1$) to provide results compatible with the strong shock assumption. Actual formulation of the relevant similarity equations is given in Ref. 9 and is based on the work of Sakurai.[14]

The shock discontinuity obtained from the similarity solution is represented initially in the numerical procedure as a step change between the two mass points straddling the actual shock location. The artificial viscosity "constant" in Eq. (25) is calculated to provide an artifical viscosity difference that approximates the pressure difference across the shock. Until the shock has propagated outward one mass point, this artificial viscosity constant is readjusted at each new time step to insure only negligible changes in shock velocity. This adjustment procedure is required to maintain stability until the shock "jump" conditions spread over several mass points. Afterwards, no additional adjustment is necessary. For the spherical problem, the artificial viscosity constant was found to increase from an initial value of approximately 1.0, as indicated in Ref. 13, to approximately 3.0 to maintain stability.

Analytical Results

Several test cases were performed using the computer program. The cases investigated were taken directly from test conditions encountered during the parallel experimental program[9] and included spherical ($\alpha = 2$) blast waves resulting from linear energy input ($\beta = 1$) for air ($\gamma = 1.4$) and chloroform ($\gamma = 1.144$). As noted in Ref. 9, chloroform was selected to facilitate data acquisition in the experimental investigation.

Typical analytical results obtained for linear energy deposition in air are presented in Figs. 2 and 3, where radial variations of density and pressure are presented. (Chloroform results are reported in Ref. 9.) Both of these figures show the presence of a piston. In each case, the curve for $\tau = 0.01$ is based on a similarity solution, and existence of a piston at this time insures existence at later times during the energy deposition period, where profiles are based on the numerical procedure. Solutions for instantaneous energy deposition[1-6] do not display this piston and hence have considerably different profiles, as shown in Figs. 4 and 5, which are based on the work of Brode.[16]

Plots of shock trajectory and shock Mach number determined from the numerical solution for linear energy input are compared with results from a similarity solution in Fig. 6. Initially, the trajectory based on the numerical solution is observed to agree with the similarity solution. At later times, when the strong shock ($M \gg 1$) assumption used in the

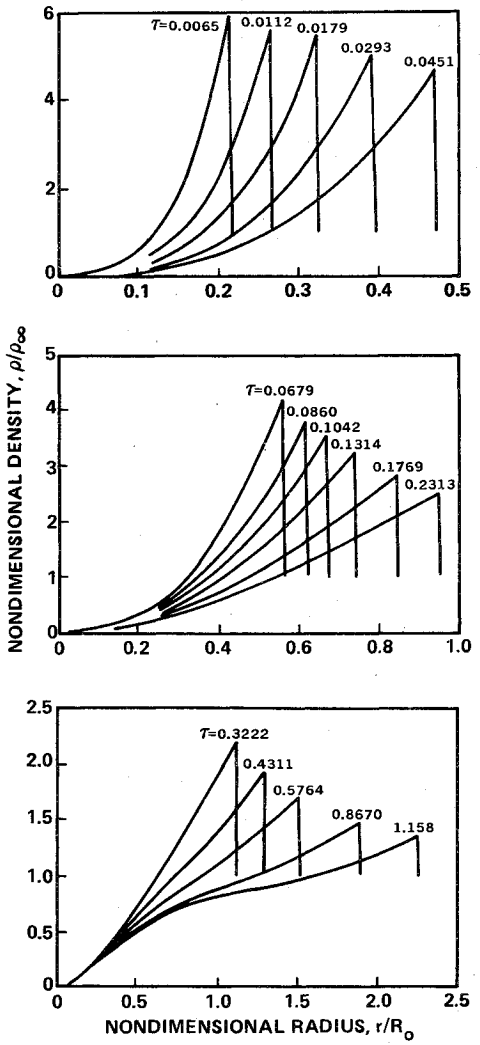

Fig. 4 Raidal density profiles for instantaneous energy input in air.

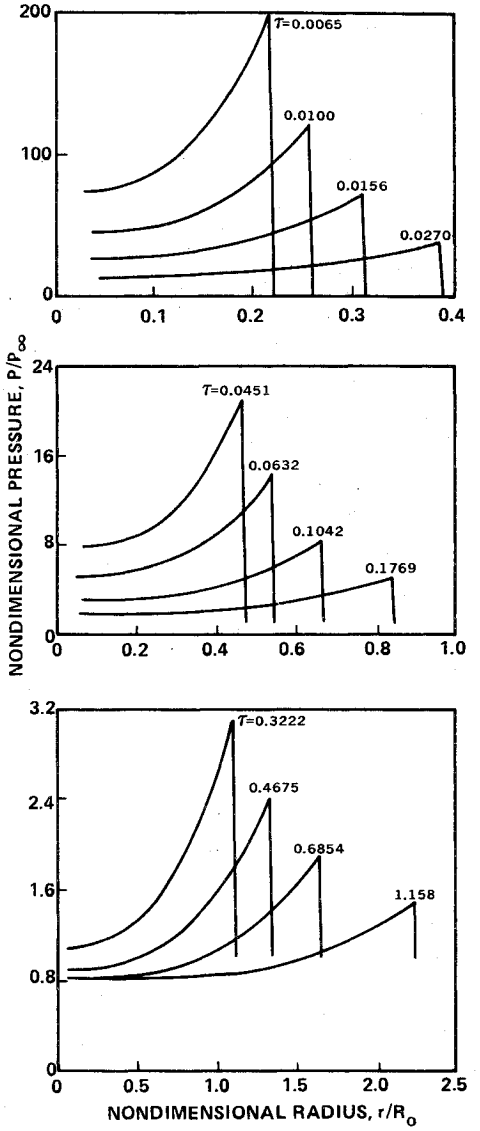

Fig. 5 Radial pressure profiles for instantaneous energy input in air.

similarity solution obviously is no longer valid, differences between the similarity solution and the numerical procedure become apparent. It should be noted that the present numerical solution provides essentially the same trajectory and shock Mach number history as the approximate solution of Dabora.[15] However, the present approach also provides detailed flowfield information such as density, pressure, and velocity which is not available from the simpler approximate procedure. The trajectory and Mach number predictions for instantaneous energy deposition, based on a similarity solution and the approximate solution of Dabora,[15] also are shown. It is observed that initially different trajectories are indicated for the two forms of energy deposition. Specifically, $R \sim t^{3/5}$ for linear energy deposition, whereas $R \sim t^{2/5}$ for instantaneous energy deposition. At later times, the trajectories for both forms of energy deposition deviate from the similarity solution and appear to approach coalescence. This gives rise to the general belief that the blast wave trajectory alone is not a good indication of the form of energy deposition unless a significant portion of the early time trajectory is available.

The nondimensional energy input time τ_i was assumed equal to unity in generating the curves of Figs. 2, 3, and 6. Dabora[12] has shown that different trajectories result when nondimensional input times other than unity are used. These differences are apparent in the top part of Fig. 7, where trajectories for $\tau_i = 0.5$ and $\tau_i = 1.0$ are shown. In order to apply the results found for one value of nondimensional input time at other values of input time, new nondimensional variables must be established such that the curves for all values of τ_i collapse to one curve. One such representation was derived during the current investigation. It uses the shock radius based on the similarity solution, which can be expressed in dimensional form:

$$R = t^{(\beta+2)/(\alpha+3)} \left[\left(\frac{\alpha+3}{\beta+2} \right)^2 \frac{E_\alpha a_\infty^2}{t_i^\beta p_\infty J_0} \right]^{1/(\alpha+3)} \tag{29}$$

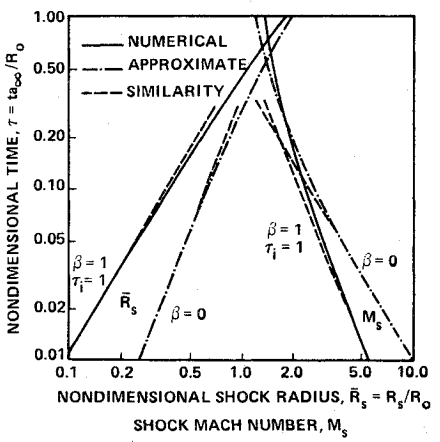

Fig. 6 Predicted shock trajectories and Mach numbers in air.

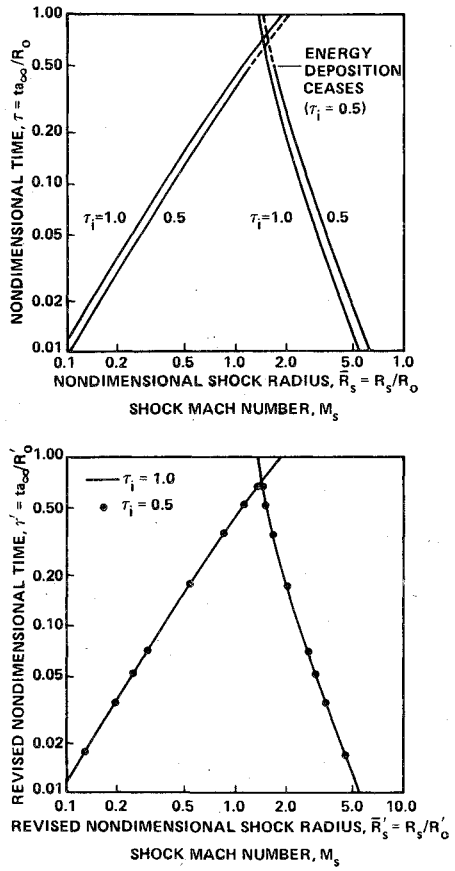

Fig. 7 Use of revised explosion scale radius to collapse curves (linear energy input in chloroform).

Equation (29) is nondimensionalized using the standard explosion scale radius:

$$\frac{R_s}{R_0} = \left(\frac{ta_\infty}{R_0}\right)^{(\beta+2)/(\alpha+3)} \left[\left(\frac{\alpha+3}{\beta+2}\right)^2 \frac{1}{J_0}\left(\frac{R_0}{t_i a_\infty}\right)^\beta\right]^{1/(\alpha+3)} \tag{30}$$

An equivalent form of Eq. (30) is desired such that the nondimensional energy input time, $\tau_i = t_i a/R_0$, is eliminated, i.e.,

$$\frac{R_s}{R_0'} = \left(\frac{ta_\infty}{R_0}\right)^{(\beta+2)/(\alpha+3)} \left[\left(\frac{\alpha+3}{\beta+2}\right)^2 \frac{1}{J_0}\right]^{1/(\alpha+3)} \tag{31}$$

Dividing Eq. (30) by Eq. (31) and rearranging provides a relationship between the original explosion scale radius R_0 and a new explosion scale radius R_0':

$$R_0' = R_0 t_i^{-[\beta/(\alpha+1-\beta)]} \tag{32}$$

A new nondimensional time and new explosion mass also must be used to apply the new explosion scale radius:

$$\tau' \equiv \frac{ta_\infty}{R_0'} = \frac{ta_\infty}{R_0}\frac{R_0}{R_0'} = \tau\frac{R_s}{R_0'} \tag{33}$$

$$m_0' \equiv \frac{F_0}{\alpha+1}\rho_\infty R_0'^{\alpha+1} = \frac{F_0}{\alpha+1}\rho_\infty R_0^{\alpha+1}\left(\frac{R_0'}{R_0}\right)^{\alpha+1} \tag{34a}$$

$$m_0' = m_0\left(\frac{R_0'}{R_0}\right)^{\alpha+1} \tag{34b}$$

The shock trajectories and Mach numbers previously calculated for $\tau_i = 0.5$ (Fig. 7a) have been recast in terms of the new explosion scale radius. They are compared with results for $\tau_i = 1.0$ in Fig. 7b. Excellent agreement is observed for nondimensional times less than the nondimensional energy input time. It appears that the results found to $\tau_i = 1$ can be applied at any other value of τ_i for the same gas by using the transformation represented by Eqs. (32-34), provided that $\tau \le \tau_i$. The transformations are not necessarily valid at nondimensional times greater than the input time, and the curves will not necessarily collapse.

Conclusions

As a result of the current investigation, the following conclusions may be drawn:

1) A numerical technique based on a Lagrangian formulation that is valid during energy deposition has been developed for predicting the trajectories and flowfield properties of variable-energy blast waves. The numerical technique uses a finite-difference formulation of the equations of motion in conservation form. It is completely general; i.e., planar, cylindrical, or spherical geometry may be specified. A prior specification of the density distribution is not required. Energy input is limited to forms that can be represented by a power law, i.e., $E \sim t^\beta$ for $0 < \beta \le \alpha + 1$, although actual checkout of the computer program has been accomplished only for linear energy deposition. The present numerical approach provides results valid over the entire energy deposition period. Its results include internal flowfield details not available to current approximate solutions, and it is not restricted to early times, such as similarity solutions that are based on a strong shock assumption.

2) Flowfield solutions and shock trajectories for air and chloroform ($\gamma = 1.4$ and 1.144, respectively) have been determined for linear energy input ($\beta = 1$) in spherical flow ($\alpha = 2$). Trajectories are observed to asymptotically approach the trajectory curves for instantaneous energy input. However, internal flowfields for the linear energy deposition cases display marked differences from flowfields for instantaneous deposition.

Acknowledgments

This research was sponsored in part by the Army Research Office under ARO-D Grant DA-ARO-31-124-73-G100. Computer time was furnished by the University of Connecticut Computer Center.

References

[1] Taylor, G.I., "The Formation of a Blast Wave by a Very Intense Explosion," *Proceedings of the Royal Society*, Ser. A, Vol. 201, March 1950, pp. 143-174.

[2] Sakurai, A., "Blast Wave Theory," *Basic Developments in Fluid Dynamics*, edited by M. Holt, Academic Press, New York, 1965, pp. 309-375.

[3] Sedov, L.I., *Similarity and Dimensional Methods in Mechanics*, Academic Press, New York, 1959, Chap. 4.

[4] Lee, J.H., Knystautas, R., and Bach, G.G., "Theory of Explosions," McGill Univ., MERL Rept. 69-10, 1969.

[5] Oppenheim, A.K., Lundstrom, E.A., Kuhl, A.L., and Kamel, M.M., "A Systematic Exposition of the Conservation Equations for Blast Waves," *Journal of Applied Mechanics*, Vol. 38, Dec. 1971, pp. 783-794.

[6] Oppenheim, A.K., Kuhl, A.L., Lundstrom, E.A., and Kamel, M.M., "A Parametric Study of Self-Similar Blast Waves," *Journal of Fluid Mechanics*, Vol. 52, Pt. 4, April 1972, pp. 657-682.

[7] Boni, A.A. and Su, F.Y., "An Analytical Technique for Laser Driven Shock Waves," *Acta Astronautica*, Vol. 1, May-June 1974, pp. 761-780.

[8] Bach, G.G. and Lee, J.H.S., "An Analytical Solution for Blast Waves," *AIAA Journal*, Vol. 8, Feb. 1970, pp. 271-275.

[9] Director, M.N., "An Investigation of Variable Energy Blast Waves," Ph.D. dissertation, Univ. of Connecticut, 1975.

[10] Director, M.N. and Dabora, E.K., "An Experimental Investigation of Variable Energy Blast Waves," *Fifth International Colloquium on Gas Dynamics of Explosions and Reactive Systems*, Bourges, France, Sept. 1975.

[11] Rogers, M.H., "Similarity Flows Behind Strong Shock Waves," *Quarterly Journal of Mechanics and Applied Mathematics,* Vol. 11, Pt. 4, Dec. 1958, pp. 411-422.

[12] Dabora, E.K., "Variable Energy Blast Waves," *AIAA Journal,* Vol. 10, Oct. 1972, pp. 1384-1386.

[13] Von Neumann, J. and Richtmeyer, R.D., "A Method for the Numerical Calculation of Hydrodynamic Shocks," *Journal of Applied Physics,* Vol. 21, March 1950, pp. 232-237.

[14] Sakurai, A., "On the Propagation and Structure of the Blast Wave, I," *Journal of the Physical Society of Japan,* Vol. 8, May 1953, pp. 662-669.

[15] Dabora, E.K., "Variable Energy Blast Wave Trajectories – Approximate Solutions," Univ. of Connecticut, Dept. of Mechanical Engineering Rept., 1973.

[16] Brode, H.L., "Numerical Solutions for Spherical Blast Waves," *Journal of Applied Physics,* Vol. 26, June 1955, pp. 766-775.

[17] Brode, H.L., Asano, W., Plemmons, M., Scantlin, L., and Stevenson, A., "A Program for Calculating Radiation Flow and Hydrodynamic Motion," The Rand Corp., Memo. BM 5187-PB, Santa Monica, Calif., April 1967.

[18] Brode, H.L., "Gas Dynamic Motion with Radiation: A General Numerical Method," *Astronautica Acta,* Vol. 14, June 1969, pp. 433-444.